

Sustainable Solutions for Energy and Environment, EENVIRO - YRC 2015, 18-20 November
2015, Bucharest, Romania

The influence of grooved surface and liquid properties on vortices formation in vicinity of immersed cylinders

Nicoleta Octavia Tanase*^a, Iulia – Rodica Damian^a, Diana Broboana^a, Corneliu Balan^a

^aUniversity "Politehnica" of Bucharest, 313 Splaiul Independentei sector 6, 060042 Bucharest, Romania

Abstract

The paper is dedicated to the experimental and numerical investigations of the viscous and viscoelastic flows around immersed cylinders with smooth and grooved surfaces. The study analyses the influences of the cylinders surface quality on the vortical structures and the wake developed downstream in a 2D open channel. The analyzed flow is in the domain of the free surface weakly turbulence regime under subcritical conditions. Numerical simulations are performed with turbulent solvers implemented in Ansys Fluent, using the VOF code for the calculation of the free surface geometry. The numerical results and visualizations are corroborated to determine the effect of the grooved surface on the drag coefficient and the location of the boundary layer separation points. The investigations emphasize also the qualitative changes of the flow spectrum induced by the Reynolds number magnitude and the presence of elasticity within the viscous fluid.

© 2016 The Authors. Published by Elsevier Ltd. This is an open access article under the CC BY-NC-ND license (<http://creativecommons.org/licenses/by-nc-nd/4.0/>).

Peer-review under responsibility of the organizing committee EENVIRO 2015

Keywords: Free surface flow; numerical simulation; flow visualizations; vortical structures

1. Introduction

The modelling of flow configuration around smooth and patterned cylinders is today a benchmark CFD domain of study in fluid mechanics, especially in relation to the boundary layer separation, wake formation and the laminar – turbulent transition [1-3].

The free surface flow around an immersed cylinder is a relatively novel subject of investigations. This particular motion, defined by two non-dimensional numbers: Reynolds and Froude, respectively

$$Re = \frac{\rho V_0 D}{\eta_0}, Fr = \frac{V_0}{\sqrt{gD}}, \quad (1)$$

is of interest for many applications from micro-fluidics to hydrology and geophysics, [1-5].

Sheridan et al. [6], was the first who investigated in details the kinematics of the flow pattern and the wake geometry downstream of the immersed cylinder, in particular the transport of vorticity flux from the free surface to the fluid domain. The experiments consisted of the velocity measurements (using the PIV technique) around the cylinder of diameter $D = 25.4$ mm immersed at different depth h in a free surface channel of width $B = 210$ mm and height at the entrance in the channel of $H_0 = 527$ mm. The ranges of Reynolds and Froude numbers were: $5990 < Re < 9120$, respectively $0.47 < Fr < 0.72$, which corresponded to an average upstream velocity within the range of $0.236 \leq V_0 \leq 0.359$ [m/s].

A direct visualization of the flow in vicinity of an immersed cylinder was presented and analyzed by Hoyt and Sellin [7]; the channel had dimensions of 102 mm width and 300 mm height, with $D = 67$ mm. The investigations were performed for six heights in the range $0 \leq h/D \leq 0.75$, but the study was focused only on three values, $h/D = 0; 0.3; 0.75$, at the same upstream average velocity, $V_0 = 0.43$ m/s.

Babu and Mahesh [8], studied the numerical simulations of the flow past cactus-shaped cylinders in the laminar regime (Reynolds numbers up to 300). The presence of grooved surface on cylinders reduce the viscous forces in comparison to a smooth cylinder for the same Reynolds number. At low Reynolds numbers the grooves create local recirculation zones, these regions have decreased surface stresses and decreased pressure forces closer to the surface. The phenomena of the decreasing drag induced by the grooves of the immersed bodies were later investigated by other authors, [2, 3, 9 - 11].

In a previous study, Tanase et al. [12], focused the analysis of the flow to the study of the interaction between the free surface and the cylinder's downstream wake, correlated with the influence of the immersed depth on the free surface geometry.

One aim of the present study is to establish the most indicated turbulence model to compute and to reproduce the flow pattern in the vicinity of an immersed cylinder for the weak turbulent subcritical flow regime, i.e. $Re < 10000$ and $Fr < 1$. Numerical simulations were performed with different turbulence solvers implemented in the Fluent code for the case of a smooth cylinder immersed in a 2D channel, the free surface geometry being computed using the VOF model. The numerical results are compared and calibrated with experiments performed with two fluids: water and weakly elastic polymer solution (small concentration of polyacrylamide in water – PAA).

The main goal of the paper is to investigate the influences of the grooved surfaces and fluids properties on the vortices formation downstream the immersed cylinders and on the location of the boundary layer detachment from the cylinders.

Nomenclature

D	diameter of the cylinder (m)
V_0	average velocity upstream the immersed cylinder (m/s)
ρ	density of fluids (kg/m^3)
η_0	viscosity of fluids ($\text{Pa}\cdot\text{s}$)
g	gravitational acceleration (m/s^2)
Re	Reynolds number (-)
Fr	Froude number (-)
B	width of channel (m)
H_0	height at the entrance in the channel (m)
Q	flow rate (m^3/s)

2. Experimental set up

The experiments are performed in an open channel, the flow rate and the fluid height upstream the smooth and grooved immersed cylinders being controlled by a weir. The average velocity upstream the cylinders of diameter $D = 50$ mm is $V_0 = Q/BH_0$, where the flow rate Q is measured by volumetric method and height $H_0 = 105$ mm is kept constant, see Fig. 1. The grooved cylinder and the detail of the grooves geometry are presented in the Fig. 2.

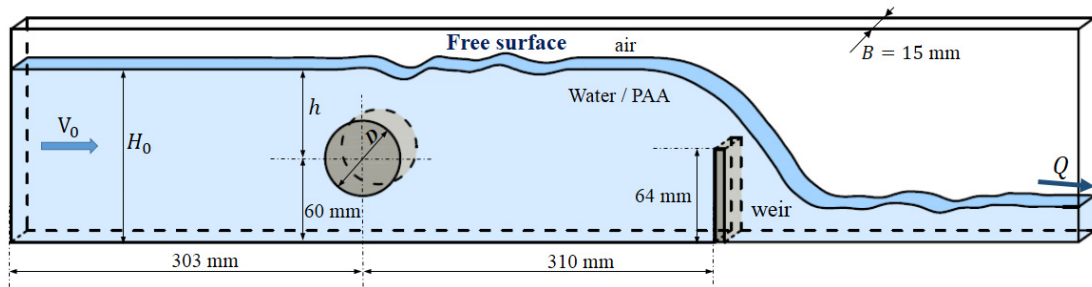


Fig. 1. The geometry of the open channel and the main geometrical characteristics. The cylinder is immersed at a depth of $h = 40.5$ mm from the upstream unperturbed free surface.

The viscosity of the two samples are $\eta_0 = 10^{-3}$ Pa·s for water and $\eta_0 = 5.6 \cdot 10^{-3}$ Pa·s for the weakly elastic polymer solution (PAA). The polyacrylamide solution PAA has a low constant viscosity and no detectable elasticity in shear rheometry measurements. For both fluids, the flows are in the region of weak turbulence ($Re = 7500$ for water, $Re = 1350$ for PAA, respectively) and $Fr < 0.5$, which corresponds to the subcritical gravitational flow regime.

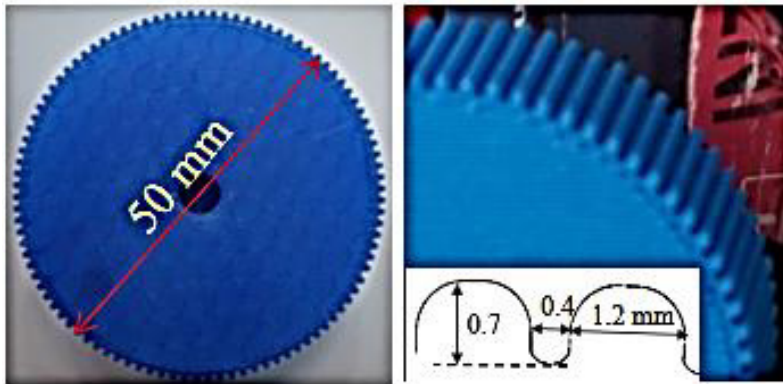


Fig. 2. The grooved cylinder fabricated using the 3D printing technology and the detail of the round tooth geometry. The teeth are uniformly and dense distributed on the surface with height $\delta = 0.7$ mm.

The direct visualizations for highlighting the vortices, wake structure and the location of critical points (D1, D2) on the immersed cylinders were obtained using a Sony SLT high resolution digital camera at 12 frames/s, Fig. 3a, [12-14].

3. Numerical simulations of the flow around immersed cylinder

The numerical analyses were focused to investigate the flow between the free surface and the wake downstream the immersed cylinders. One important parameter is the position of the separation/critical points on the wall, where the boundary layer detached from the cylinder's surface. Location of the separation points and the wake pattern (in addition to the trace of the free surface line, see for details [13]) are the main characteristics used to correlate the experiments with numerics.

The turbulence models used for the numerical simulations of free surface flow around an immersed smooth cylinder were: (i) $k - \varepsilon$ standard with Standard Wall Functions (case C1), (ii) $k - \varepsilon$ RNG with Standard Wall Functions (case C2), (iii) $k - \varepsilon$ RNG with RNG - options: Differential Viscosity Model (case C3), (iv) $k - \varepsilon$ realizable with Standard Wall Functions (case C4), (v) $k - \omega$ standard with options Shear Flow Corrections (case C5) and (vi) Transitional Flows (case C6), [15-17].

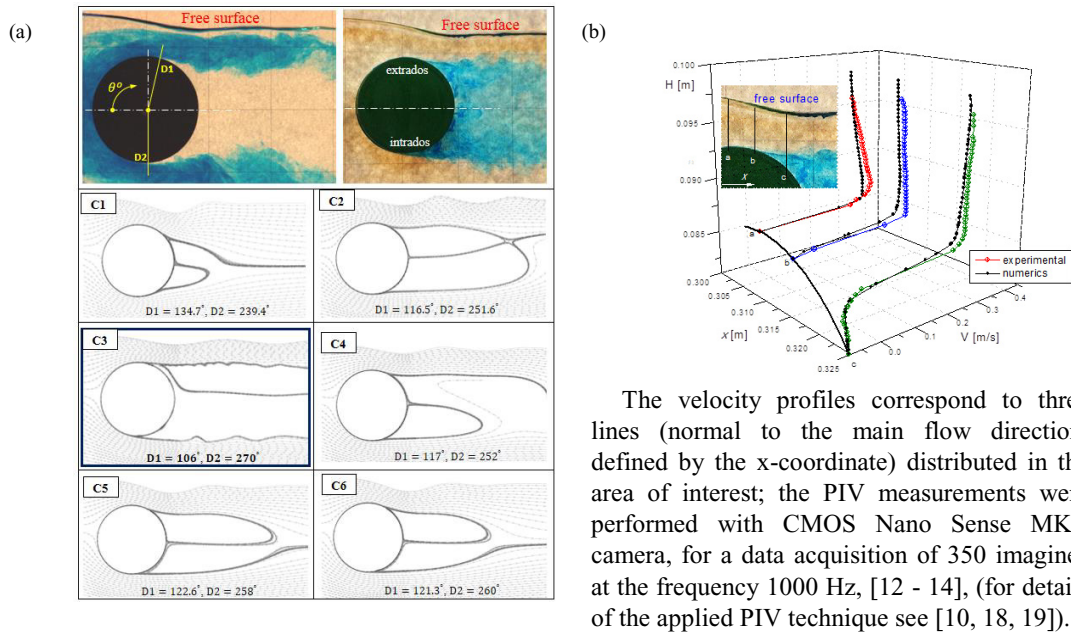


Fig. 3. (a) Comparison of the numerical and experimental flow spectrum and the position of the separation points of the boundary layer from the cylinder. (b) Comparison between measured and computed velocity distributions in the region between the cylinder and the free surface.

In the Fig. 3a are presented the results corresponding to the tested turbulence models for the flow spectrum and the location of the separation points D1 and D2, defined as the points on the extrados, respectively intrados, of the cylinder where the boundary layer detaches from the surface, [12]. The experimental visualizations of the wake and the measured position of the separation points are also shown.

The experimental separation points D1 and D2 are located at the angles $\theta_1 \cong 107^\circ$, $\theta_2 \cong 271^\circ$, values obtained from direct visualizations of the boundary layer detachment. The numerical values of θ_1 and θ_2 , which correspond to the location where the wall shear stress is zero, are computed directly from the numerical solutions, for details see [20]. The best fitting of experimental values of the angles θ_1 and θ_2 are given by solution C3. A quantitative confirmation that solution C3 is the most indicated for the analysis is obtained by the comparison of the measured and computed velocity profiles between the immersed cylinder and the free surface shown in Fig. 3b, where the results are found very satisfactory.

In conclusion, the analysis of the free surface hydrodynamics around immersed smooth and grooved cylinders will be performed based on the 2D case C3 numerical simulations, the $k - \varepsilon$ RNG model for turbulence (coupled with the VOF model) being the best available choice for representing the flow configuration under study.

We have to remark that numerical computations were performed with Newtonian incompressible viscous models for both samples, so the elasticity was not present in the computations which correspond to the PAA fluid.

3.1. Comparison between smooth and grooved immersed cylinders

A cylinder with grooved surface was investigated under the same conditions as the smooth cylinder. The groove has a round tooth geometry with small aspect ratio $\bar{\delta} = \delta/D = 0.014$; the grooves are uniformly distributed on the cylinder of nominal diameter $D = 50$ mm, see Fig. 2. The flows around the smooth and grooved cylinders are shown in Fig. 4, where the numerical pathlines were overlapped on the direct visualisations of the flow patterns. For the tested range of the Reynolds numbers, experimental visualizations and numerical computations were in agreement with the statement that grooved surface doesn't change significantly the position of the detachments points in comparison to the smooth cylinder.

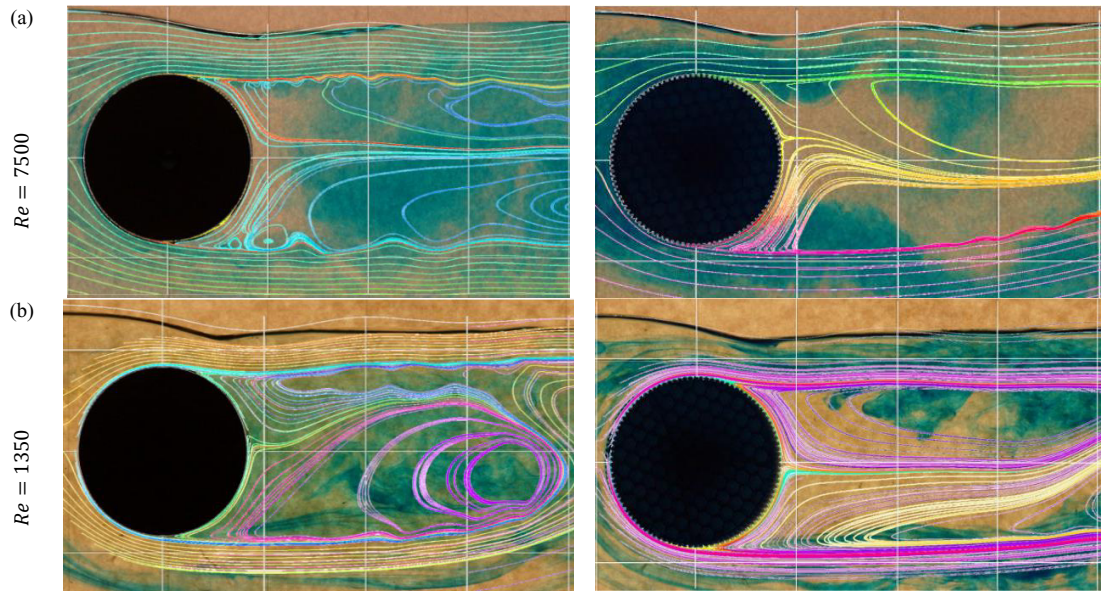


Fig. 4. Comparison between smooth and grooved cylinders for (a) water and (b) PAA cases: experimental and computed flow spectrum. The numerics reproduce well the recorded pathlines and the downstream wake.

In Fig. 5 the distributions of the computed pressure and the vorticity on the circle tangent to the grooved cylinder for water ($Re = 7500$) and PAA ($Re = 1350$) are plotted. The fluctuations of vorticity ω , the wake region and the separation points are marked in Fig.5b, where the decreasing of vorticity fluctuations and magnitude was observed for low value of the Reynolds number. In Fig. 6 are direct compared the distributions of turbulent viscosity on circles of radius $R1 = 26.6$ mm and $R2 = 34.6$ mm for the grooved cylinder. The regions with high values of turbulent viscosity (proportional to the ratio between the square of turbulent kinetic energy k and turbulent dissipation ϵ) are observed between the free surface and the extrados of the immersed cylinder. The decreasing of turbulent viscosity takes place in vicinity of the separation points and indicates the detachment of the shear-layers vorticity, Fig. 6a. The distribution is almost symmetric at $Re = 7500$ in the very vicinity of the cylinders at radius $R1$, where turbulence is almost absent for $Re = 1350$. At radius $R2$ the turbulent viscosity is increasing (here the values are similar for both Reynolds numbers) but the vorticity is more present in the extrados domain, where turbulent viscosity is larger than at the intrados of the cylinder, Fig. 6b.

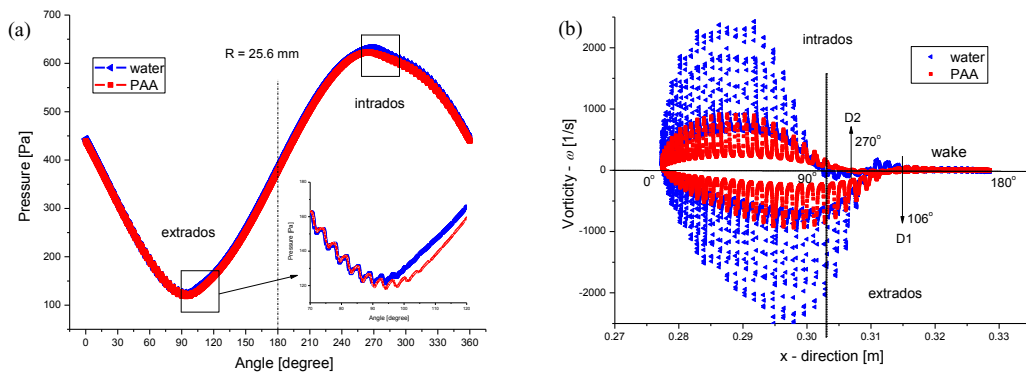


Fig. 5. Distributions of the pressure (a) and vorticity (b) on the circle tangent to grooved-cylinder for water and PAA. The pressure difference is not remarkable between the two cases, but the vorticity magnitude is decreasing with decreasing the Reynolds number.

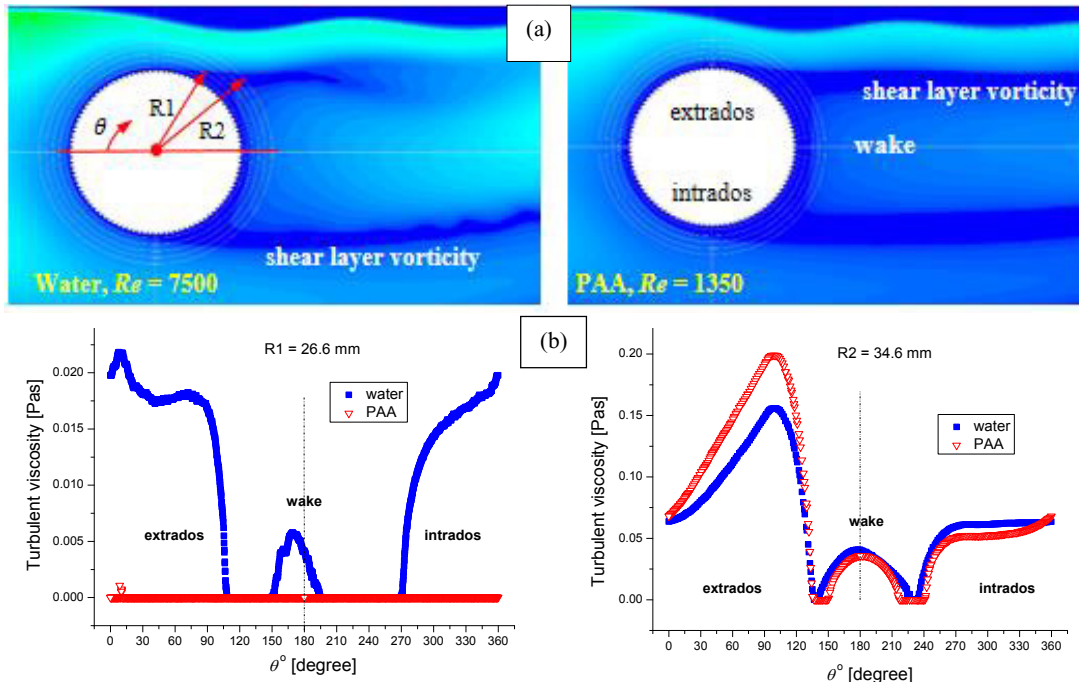


Fig. 6. (a) Distribution of turbulent viscosity, (b) comparison between water and PAA for turbulent viscosity on different circles radius from the grooved cylinder.

The distributions of the computed apparent wall stress ($WSS := \eta_0 \omega$) on the groove surface are shown in Fig. 7. The location of the detachment point corresponds to zero wall stress; the point D1 is located for PAA case at tooth W7, instead at W5 as for the water, the moving downstream of D1 being determined by the decreasing of the Re -number, [24]. The distributions of the WSS show the differences the local hydrodynamics of the two liquids. The values of WSS are larger for the PAA case, which is determined by the increasing of viscosity over the decreasing of vorticity with decreasing the Reynolds number, see Fig. 5b.

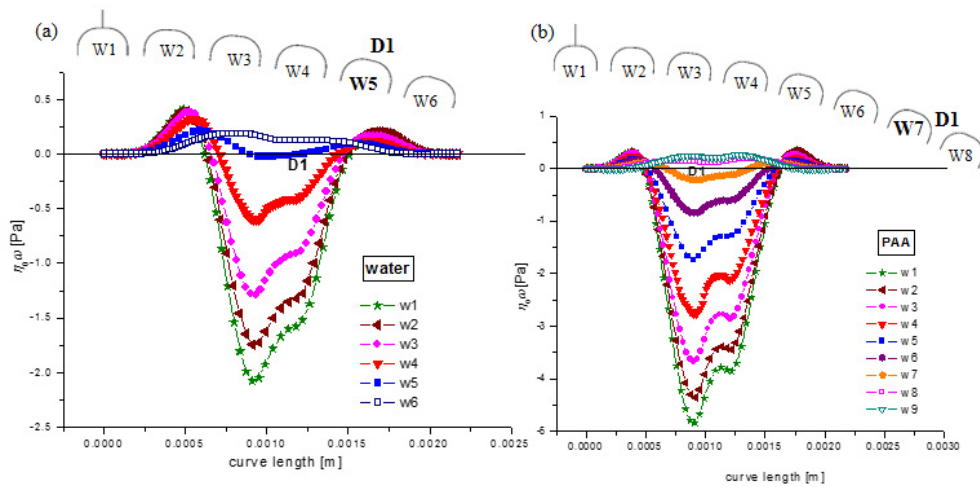


Fig. 7. Computed distributions of the WSS along the surface of the grooved for water, $Re = 7500$ (a) and PAA, $Re = 1350$ (b).

The numerical results and visualizations are corroborated to determine the influence of fluid elasticity. In Fig. 8a the computed results for water at $Re = 7500$ are perfectly correlated with the visualizations, the location of D1 being at the same tooth, respectively W5, for numerics and experiments. This is not the case for $Re = 1350$, see Fig. 8b, where the pure viscous solution is compared with experiments performed with PAA. In both cases the Re value is the same, but in experiments the presence of elasticity might induce changes in the flow spectrum. As can be observed the location of D1 corresponds in numerics at W7 and in experiments at W8. These results confirm that a small amount of elasticity postpone the onset of flow separation from the solid surfaces, without to have any effect far from the walls where the flow is dominated by the shear components [21].

In this case the presence of grooves on cylinder surface doesn't influence significantly the position of separation point, and as a consequence also the total drag force, see Table 1. But the computations prove that the patterned surface reduces the viscous (friction) force over the immersed body in comparison to the smooth surface, result which is in agreement with the findings of the previous studies, [8, 11, 22-23].

Table 1. The values of the components of the drag forces acting on the cylinders calculated from the numerical solutions

Cylinders - fluids	Pressure force [N]	Viscous force [N]	Total force [N]	Pressure coefficient [-]	Viscous coefficient [-]	Total coefficient [-]
smooth - water	2.0686	0.0441	2.1127	3.3774	0.07198	3.4494
smooth - PAA	2.0764	0.1163	2.1928	3.3901	0.18998	3.5801
grooved - water	2.0879	0.0276	2.1155	3.4088	0.0451	3.454
grooved - PAA	2.2239	0.08083	2.30322	3.62839	0.13197	3.76037

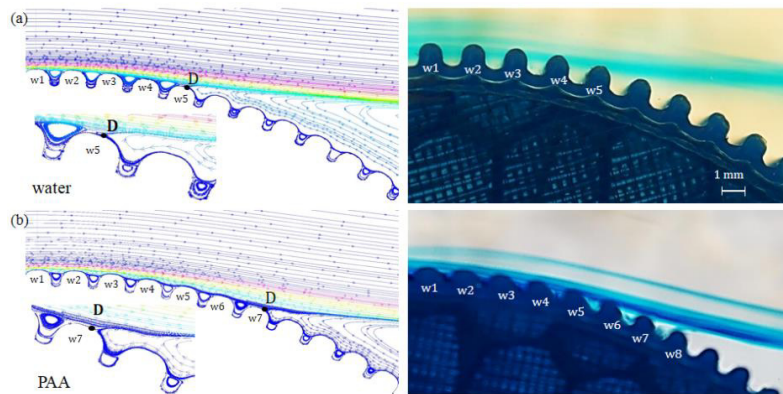


Fig. 8. Numerical computations and direct visualization of the flow in vicinity of the separation point located on the extrados of the grooved cylinder for water (a) and PAA (b).

4. Conclusions

The free surface channel flow in vicinity of immersed smooth and grooved cylinders was studied for weakly turbulent flow in subcritical regime. Numerical simulations for viscous fluids performed with the turbulent model $k - \epsilon$ RNG were correlated with the direct visualizations of the flow spectrum for two different samples: different samples: water and a weakly elastic polymer solution (PAA). The modelling of the free surface geometry and the study of the interaction between the wake and the free surface were presented in some previous papers of the authors [12-13].

The main goals of the present work was to investigate the influence of the grooved surface on the flow in vicinity of the separation points and to what extent the patterned surface influence the drag and friction force. The correlation between experiments and computations were very good for both smooth and grooved cylinders for water (a pure viscous fluid) at $Re = 7500$.

Decreasing the Reynolds number from $Re = 7500$ (water) to $Re = 1350$ (PAA) the computed viscous force and the viscous coefficient are increasing, result which is expected for the Newtonian fluids, [24]. The influence of the fluid elasticity is remarkable in the region of the separation point D1 on the grooved cylinder surface, where to extensional components of flow are more present in comparison with the bulk domain dominated by shear. A small amount the elasticity within the viscous fluid influences the flow spectrum in the neighbourhood of the wall by moving the separation point downstream the cylinder.

The present results are part of a CFD analysis developed in the REOROM laboratory dedicated to the modelling of flows around immersed bodies in vicinity of a separation surface. In this case the separation surface is between a liquid (water or polymer solution) and air, but in the future the investigations will be focus to the study of the influence induced by a liquid-liquid interface. The effect of grooved surface and liquid properties (viscosity, elasticity) were analyses and correlated with numerics. In the absence of a numerical solution for a viscoelastic fluid, the Newtonian solution is capable to reproduce fair the viscoelastic flow spectrum, with exception of the domains where the extensional components of stretching are present.

Our investigations confirm qualitatively and quantitatively the previous results published in literature for immersed smooth of grooved cylinders in Newtonian flows. The experiments performed with polymer solutions in the presence of a separation surface are new and will be extended in our further studies at low and very low Reynolds numbers. We are looking to focus the study to the applications in the domain of microfluidics, where the influence of patterned surface of the immersed bodies on the flow spectrum is expected to be remarkable in confined micro-geometries.

Acknowledgements

The work of Nicoleta Octavia Tanase and Iulia - Rodica Damian has been funded by the Sectoral Operational Programme Human Resources Development 2007-2013 of the Ministry of European Funds through the Financial Agreement POSDRU/159/1.5/S/132395 and POSDRU/159/1.5/S/132397. The authors acknowledge the financial support received from the grant UEFISCDI project PN-II-ID-PCE-2012-4-0245/2013 and PN-II-PT-PCCA-2011-3.1-0052. The assistance and support of associate professor Ilinca Nastase (UTCM) in obtaining the PIV measurements is also acknowledged.

References

- [1] Lee S.J., Daichin, Flow past a circular cylinder over a free surface: Interaction between the near wake and the free surface deformation, *J. Fluids and Struct.* (2004), 19: 1049–1059.
- [2] El-Makdah A.M., Oweis G.F. The flow past a cactus-inspired grooved cylinder. *Exp. Fluids* 2013, 54: 1-16.
- [3] Liu Y.Z., Shi L.L., Yu J. TR-PIV measurement of the wake behind a grooved cylinder at low Reynolds number. *J. Fluids Struct.* 2011, 27(3): 394–407.
- [4] Baum M. J., Heepe L., Fadeeva E., Gorb S. N.. Dry friction of microstructured polymer surfaces inspired by snake skin, *Beilstein J. Nanotechnol.* 2014, 5: 1091–1103.
- [5] Zheng W., Wang L.-P., Or D., Lazousskaya V., Jin Y. Role of Mixed Boundaries on Flow in Open Capillary Channels with Curved Air–Water Interfaces. *Langmuir* 2012, 28: 12753–12761
- [6] Sheridan, J., Lin, J.-C., Rockwell, D. Flow past a cylinder close to a free surface. *J. Fluid Mech.* 1997, 330: 1–30.
- [7] Hoyt J.W., Sellin R.H.J. A comparison of tracer and PIV results in visualizing water flow around a cylinder close to the free surface. *Exp. Fluids* 2000, 28(3): 261–265.
- [8] Babu P., Mahesh K. Aerodynamic loads on cactus-shaped cylinders at low Reynolds numbers. *Phys. Fluids* 2008, 20: 1-9.
- [9] Zhang HL, Ko NWM. Numerical analysis of incompressible flow over smooth and grooved circular cylinders. *Comput Fluids* 1996; 25: 263-281.
- [10] Abboud J.E., Karaki, W.S. Oweis, G.F. Particle image velocimetry measurements in the wake of a cactus-shaped cylinder. *J. Fluids Eng.* 2011, 133 (9): 1-3.
- [11] Yamagishi Y, Oki M. Effect of groove shape on flow characteristics around a circular cylinder with grooves. *J Vis* 2004; 7(3): 209–216.
- [12] Tanase NO, Broboana D, Balan C. Free surface flow in vicinity of an immersed cylinder. *Proc Rom Acad Ser A* 2014; 15: 371–378.
- [13] Tanase NO, Broboana D, Balan C. Flow around an immersed cylinder in the presence of free surface. *UPB Sci Bull Ser D: Mech Eng* 2014; 76: 259–266.

- [14] Tanase NO. Hydrodynamics of free surface flow in vicinity of immersed bodies in transitory subcritical flow regim (in Romanian). University “Politehnica” of Bucharest; 2013.
- [15] Danaïla S, Berbente C. Numerical methods in fluid dynamics (in Romanian). Ed Academiei, Bucuresti; 2003.
- [16] Launder BE, Spalding DB. Mathematical models of turbulence. In: Academic Press, London; 1972.
- [17] Ansys Inc. Ansys Fluent Theory Guide 2013.
- [18] Sheridan J, Lin J, Rockwell D. Metastable states of a cylinder wake adjacent to a free surface. *Phys Fluids* 1995; 7 (9): 2099–2101.
- [19] Nastase I, Meslem A. Vortex dynamics and entrainment mechanisms in low Reynolds orifice jets. *J Vis* 2008; 11 (4): 309-318.
- [20] Tanase, N. O., Broboana, D., Balan, C., 2015. Numerical and experimental investigations of the flow configuration in vicinity of immersed smooth and patterned cylinders. *Proc. Rom. Acad. Ser. A*, in press.
- [21] Broboana D., Muntean T., Balan C. Experimental and numerical studies of weakly elastic viscous fluids in a hele – shaw geometry. *Proc Rom Acad Ser A* 2007; 8(3): 219-233.
- [22] Munendra CV, Inamdar A, Kumar R. Numerical Studies of Drag reduction on Circular Cylinder With V- Grooves. *Int J Eng Gen Sci* 2015; 3 (3): 290–302.
- [23] Wang SF, Liu YZ, Zhang QS. Measurement of flow around a cactus-analogue grooved cylinder at $Re_D = 5.4 \cdot 10^4$: Wall-pressure fluctuations and flow pattern. *J Fluids Struct* 2014; 50: 120–136.
- [24] Schlichting H, Gersten K. *Boundary-Layer Theory*. In: Springer, Berlin; 2000.